Polym. Bull. (2015) 72:653–669
DOI 10.1007/s00289-014-1284-1

REVIEW

Novel D–π–A dye sensitizers of polymeric metal complexes with triphenylamine or carbazole derivatives as donor for dye-sensitized solar cells: synthesis, characterization and application

Dahai Peng · Guipeng Tang · Jiaomei Hu · Qiufang Xie · Jun Zhou · Wei Zhang · Chaofan Zhong

Received: 22 March 2014 / Revised: 16 October 2014 / Accepted: 27 November 2014 /
Published online: 6 December 2014

Abstract In this paper, four novel D–π–A polymeric metal complexes as dye sensitizers for dye-sensitized solar cell, which have triphenylamine or carbazole derivative used as an electron donor (D), C=C bond used as π-bridge (π), and transition metal complexes used as an electron acceptor (A), were synthesized and characterized. They have been determined and studied by FT-IR, thermogravimetric analyses, differential scanning calorimetry, gel permeation chromatography, elemental analysis, UV–Vis absorption spectroscopy, photoluminescence spectroscopy, cyclic voltammetry, *J–V* curves and photon-to-electron conversion efficiency plots. Polymeric metal complexes which have carbazole derivatives used as an electron donor (D) and cadmium used as coordination metal ion exhibited better power conversion efficiency (η) than the other polymeric metal complexes. The dye-sensitized solar cells (DSSCs) fabricated by PBL1 exhibit good device performance with a power conversion efficiency of up to 1.76 % ($J_{sc} = 4.74$ mA/cm^2, $V_{oc} = 0.63$ mV) under simulated AM 1.5 G irradiation indicating that the polymeric metal complexes are promising in the development of DSSC.

Keywords Dye sensitizer · Polymeric metal complex · Triphenylamine · Carbazole

Introduction

In recent years, the energy resource has become an urgent problem to be solved for the whole world. Solar cells are regarded as one key technology to use solar energy, which is one of the wonderful energy resources [1]. Huge efforts have been invested

D. Peng · G. Tang · J. Hu · Q. Xie · J. Zhou · W. Zhang · C. Zhong (✉)
Key Laboratory of Environmentally Friendly Chemistry and Applications of Ministry of Education, College of Chemistry, Xiangtan University, Xiangtan 411105, Hunan, China
e-mail: zhongcf798@aliyun.com

for seeking the better photovoltaic materials to take advantage of solar irradiation (5 % UV, 43 % visible, 52 % IR) efficiently [2]. Compared to the conventional silicon-based semiconductor photovoltaic devices, which were first reported in 1991 by O'Regan and Grätzel [3], dye-sensitized solar cells (DSSCs) are becoming more attractive for their numerous potential advantages such as low cost, large-area capability and easy processing. Among the key components of a DSSC, the sensitizer always plays as one of the most crucial elements since it exerts a significant influence on the power conversion efficiency (η) as well as the device stability. To date, ruthenium complex-sensitized DSSCs have reached η values of more than 11 %, whereas zinc-porphyrin co-sensitized DSSCs have reaped η of 12.3 % [4].

Compared to the ruthenium metal complex sensitizers, alternative metal-free organic sensitizers have attracted much attention because of their unique advantages, such as low cost, tunable absorption and electrochemical properties via suitable molecular design [5]. But organic small molecule dyes are less stable than metal complexes dyes, which can cause the formation of excited triplet states and unstable radicals under light irradiation. In comparison with metal-free organic small molecule dyes, conjugated organic polymer dyes hold large absorption coefficient, tunable band gap and good stability. Some of them have been used as photosensitizers in DSSCs [6]. So, finding cheap substitute metals and macromolecular structure seems very important. As a kind of the plurality of polymers, polymeric metal complexes have received considerable attention for these hybrid materials providing outstanding physical and chemical properties of both organic and inorganic components, such as unique process ability and easy film forming ability of polymer, prominent luminescence efficiency and good thermal stability of metal [7, 8]. Although the synthesis of polymeric metal complexes has been widely reported, articles about their application in dye-sensitized solar cells are quite limited. Therefore, it is worth synthesizing new polymeric metal complexes and studying their photovoltaic properties.

According to the above-mentioned points, we have designed and synthesized four D–π–A dyes possessing transition metal complexes as an acceptor (A), C=C bond as a π-conjugation linkage (π), and triphenylamine or carbazole derivatives as donor group (D), which are shown in Scheme 1. Moreover, thermal properties, optical properties and photovoltaic properties of polymeric metal complexes are also investigated in this paper.

Experimental

Materials

All starting materials were obtained from Sigma-Aldrich Chemical Co. and used without further purification. All solvents used in this work were of analytical grade. *N*, *N*-Dimethylformamide (DMF) was dried by distillation over CaH_2, and tetrahydrofuran (THF) was dried by distillation over sodium. Triethylamine was

Scheme 1 Chemical structures of PAL1, PAL2, PBL1 and PBL2

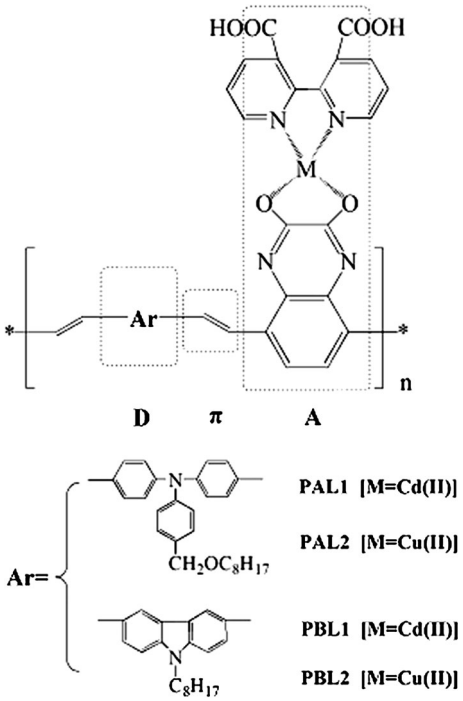

purified by distillation over KOH. The other materials were of common commercial grade and used as received.

Instrument and measurements

^{1}H NMR spectra were obtained in $CDCl_3$ and recorded with a Bruker ARX400 (400 MHz) Germany and using tetramethylsilane (0.00 ppm) as the internal reference. FT-IR spectra were recorded using KBr pellets with a Perkin-Elmer Spectrum One FT-IR spectrometer over the range 450–4,000 cm^{-1}. Gel Permeation Chromatography (GPC) analyses were measured by a WATER 2414 system equipped with a set of HT_3, HT_4 and HT_5, 1-Styragel columns with THF as eluent and polystyrene as standard. Thermogravimetric analyses (TGA), differential scanning calorimetry (DSC) and elemental analysis were performed on Shimadzu TGA-7 Instrument, Perkin-Elmer DSC-7 thermal analyzer and Perkin-Elmer 2400 II instrument, respectively. UV–visible spectra of all the polymers were taken on a Lambda 25 spectrophotometer. Photoluminescent spectra (PL) were taken on a Perkin-Elmer LS55 luminescence spectrometer with a xenon lamp as the light source. Cyclic voltammetry (CV) was conducted on a CHI630C electrochemical workstation using a three-electrode system, in a $[Bu_4N]BF_4$ (0.1 M) DMF solution at a scan rate of 50 mV/s. The working electrode was a glassy carbon electrode, the auxiliary electrode was a platinum wire electrode, and a saturated calomel electrode (SCE) was used as reference electrode.

Synthesis

Synthesis of 4-(N,N-diphenylamino)benzaldehyde ***(1)*** *[9]*

5.00 g (20.38 mmol) of triphenylamine was reacted with 40.0 mL of *N,N*-dimethylformamide (DMF) in the presence of 15.0 mL of phosphorus oxychloride ($POCl_3$) by mixing the first two reactants and adding the latter dropwise with stirring while cooling the reaction vessel in an ice bath. The mixture was refluxed for about 1 h, then poured into ice water, neutralized with 40 % sodium hydroxide (NaOH), and the product obtained by filtration. The crude product was purified through column chromatography on silica gel using chloroform/petroleum benzine (1:3 v/v) as eluent. Bright yellow crystals with yield 80 % (4.46 g) and mp 130–131 °C were obtained. FT-IR (KBr, 4,000–450 cm^{-1}): 3,037 (=C–H), 2,740 (formyl C–H), 1,690 (C=O). ^{1}H NMR (400 MHz, $CDCl_3$) δ (ppm): 9.84 (1H, *s*), 7.70 (2H, *d*), 7.37 (4H, *q*), 7.22 (2H, *d*), 7.20 (2H, *q*), 7.04 (4H, *d*).

Synthesis of [4-(diphenylamino)phenyl]methanol ***(2)*** *[10]*

[4-(Diphenylamino)phenyl]methanol **2** was synthesized by reduction of compound **1** with sodium borohydride ($NaBH_4$). 0.29 g (7.66 mmol) of $NaBH_4$ dissolved in 15.0 mL of aqueous 0.1 M NaOH solution was added dropwise into 4.01 g (14.67 mmol) of compound **1** in 50.0 mL of ethanol. The mixture was reacted at room temperature for 4 h. The solution was extracted with CH_2Cl_2–H_2O, dried with magnesium sulfate ($MgSO_4$) and then rotary evaporated. Recrystallization with dichloromethane-hexane gave a white solid. The yield was 85 % (3.43 g). FT-IR (KBr, 4,000–450 cm^{-1}): 3,432 (O–H), 3,032 (=C–H), 2,930, 2,877 (C–H). ^{1}H NMR (400 MHz, $CDCl_3$) δ (ppm): 7.27–7.02 (14H, *m*), 4.67 (2H, *s*), 2.08 (1H, *s*). Anal. calcd for $C_{19}H_{17}NO$: C, 82.88; H, 6.22; N, 5.09; found: C, 82.72; H, 6.24; N, 5.14.

Synthesis of 4-(octyloxymethyl)-N,N-diphenylbenzenamine ***(3)***

A flask was charged with a mixture of compound **2** (2.00 g, 7.26 mmol), 1-bromooctane (1.45 g, 7.51 mmol), sodium hydride (NaH) (0.53 g, 22.08 mmol) and tetrahydrofuran (THF) (50 mL). Then the flask was pumped into a vacuum and purged with N_2. The mixture was reacted at room temperature for 24 h. After that, the solution was extracted with CH_2Cl_2–H_2O, dried with magnesium sulfate ($MgSO_4$) and then rotary evaporated. The crude product was purified through column chromatography on silica gel using dichloromethane/petroleum benzine (1:1 v/v) as eluent. Pale yellow liquid with yield 78 % (2.20 g) was obtained. FT-IR (KBr, 4,000–450 cm^{-1}): 3,034 (=C–H), 2,925, 2,853 (C–H), 1,101 (C–O). ^{1}H NMR (400 MHz, $CDCl_3$) δ (ppm): 7.23–6.99 (14H, *m*), 4.43 (2H, *s*), 3.43 (2H, *t*), 1.85–0.87 (15H, *m*). Anal. calcd for $C_{27}H_{33}NO$: C, 83.68; H, 8.58; N, 3.61; found: C, 83.63; H, 8.54; N, 3.67.

*Synthesis of 3-(octyloxymethyl)-3′,3″-(diformyl)triphenylamine **(4)** [11]*

$POCl_3$ (10 mL) and DMF (20 mL) were mixed in ice bath and then a solution of compound **3** (2.00 g, 5.16 mmol) in 20 mL of 1,2-dichloroethane was added dropwise within 20 min. The mixture was refluxed for 24 h, then poured into ice water, and neutralized using saturated aqueous NaOH (adjust the pH 6–8). The solution was extracted three times with $CHCl_3$, and then dried using magnesium sulfate over night. The solvent was removed in vacuo. The residue was purified by flash column chromatography [dichloromethane/petroleum benzine (4:1 v/v) as the eluent] to get brown viscous liquid of compound **4**. Yield 60 % (1.37 g). FT-IR (KBr, 4,000–450 cm^{-1}): 3,033 (=C–H), 2,923, 2,854 (C–H), 2,733 (formyl C–H), 1,681 (C=O), 1,076 (C–O). ^{1}H NMR (400 MHz, $CDCl_3$) δ (ppm): 9.80 (2H, *s*), 7.68 (4H, *d*), 7.34–7.17 (6H, *m*), 7.01 (2H, *d*), 4.61 (2H, *s*), 3.25 (2H, *s*), 1.75–0.87 (15H, *m*). Anal. calcd for $C_{29}H_{33}NO_3$: C, 78.52; H, 7.50; N, 3.16; found: C, 78.43; H, 7.58; N, 3.22.

*Synthesis of 4-(octyloxymethyl)-N,N-bis(4-vinylphenyl)benzenamine **(A)** [12]*

0.88 g (7.80 mmol) of t-BuOK was reacted with methyltriphenylphosphonium bromide (Ph_3PCH_3Br) 3.00 g (7.40 mmol) and anhydrous THF (60 mL) by mixing the first two reactants and adding the latter with stirring while cooling the three-necked flask reaction vessel in an ice–salt bath. Then the flask was pumped into a vacuum and purged with N_2. The mixture was stirred at room temperature for 30 min. After that, the solution was added compound **4** (1.33 g, 3.00 mmol). The mixture was reacted at room temperature for 24 h and then poured into water. The solution was extracted three times with ether, and then dried using magnesium sulfate over night. The solvent was removed in vacuo. The residue was purified by flash column chromatography (dichloromethane/petroleum benzine (2:3 v/v) as the eluent) to get light color viscous solid of compound **A**. Yield 51 % (0.67 g). FT-IR (KBr, 4,000–450 cm^{-1}): 3,035 (=C–H), 2,929, 2,861 (C–H), 1,641 (C=C). ^{1}H NMR (400 MHz, $CDCl_3$) δ (ppm): 7.69 (4H, *d*), 7.33–7.16 (6H, *m*), 7.03 (2H, *d*), 6.51 (2H, *t*), 5.57 (2H, *d*), 5.14 (2H, *d*), 4.60 (2H, *s*), 3.48 (2H, *s*), 1.64–0.88 (15H, *m*). Anal. calcd for $C_{31}H_{37}NO$: C, 84.69; H, 8.48; N, 3.19; found: C, 84.21; H, 8.53; N, 3.16.

*Synthesis of N-octyl-carbazole **(5)** and N-octyl-3,6-diformyl-carbazole **(6)***

N-Octyl-carbazole **(5)** was synthesized according to the published literature [13, 14]. The product yield was 6.82 g (86 %) of white crystal. ^{1}H NMR (400 MHz, $CDCl_3$) δ (ppm): 8.14 (2H, *d*), 7.51–7.47 (4H, *m*), 7.28 (2H, *q*), 4.33 (2H, *t*), 1.91 (2H, *m*), 1.41–1.28 (10H, *m*), 0.88 (3H, *t*).

N-Octyl-3,6-diformyl-carbazole **(6)** was synthesized according to the published literature [14, 15]. A gray yellow solid 2.85 g (54 %) was gained. ^{1}H NMR (400 MHz, $CDCl_3$) δ (ppm): 10.16 (2H, *s*), 8.69 (2H, *s*), 8.11 (2H, *d*), 7.58 (2H, *d*), 4.39 (2H, *t*), 1.91 (2H, *m*), 1.38–1.20 (10H, *m*), 0.82 (3H, *t*).

*Synthesis of N-octyl-3,6-divinyl-carbazole **(B)***

The *N*-octyl-3,6-divinyl-carbazole **(B)** was synthesized according to the published literature [16]. Compound **6** can be transformed into *N*-octyl-3,6-divinyl-carbazole by a simple Wittig reaction using methyltriphenylphosphonium bromide (CH_3-PPh_3Br) in the presence of NaH in anhydrous THF to give compound **B**. Yield 69 % (0.84 g). FT-IR (KBr, 4,000–450 cm^{-1}): 3,052 (=C–H), 2,922, 2,845 (C–H), 1,635 (C=C). ^{1}H NMR (400 MHz, $CDCl_3$) δ (ppm): 7.74 (2H, *s*), 7.59–7.47 (4H, *m*), 6.90 (2H, *t*), 5.81 (2H, *d*), 5.24 (2H, *d*), 4.38 (2H, *t*), 1.89 (2H, *m*), 1.33–1.24 (10H, *m*), 0.87 (3H, *t*). Anal. calcd for $C_{24}H_{29}N$: C, 86.96; H, 8.82; N, 4.23; found: C, 86.79; H, 8.97; N, 4.19.

*Synthesis of 4,7-dibromo-2,1,3-benzothiadiazole **(7)** and 3,6-dibromo-1,2-benzenediamine **(8)***

4,7-Dibromo-2,1,3-benzothiadiazole **(7)** was synthesized according to the published literature [17]. The product yield was 5.21 g (87 %) of pale yellow crystal. FT-IR (KBr, 4,000–450 cm^{-1}): 3,089, 3,049 (=C–H), 1,594 (C=C). ^{1}H NMR (400 MHz, $CDCl_3$) δ (ppm): 7.73 (2H, *s*).

3,6-Dibromo-1,2-benzenediamine **(8)** was synthesized according to the published literature [17]. The product yield was 4.63 g (91 %) of ivory solid. FT-IR (KBr, 4,000–450 cm^{-1}): 3,332 (N–H), 3,088, 3,049 (=C–H), 1,641 (C=C). ^{1}H NMR (400 MHz, $CDCl_3$) δ (ppm): 6.85 (2H, *s*), 3.90 (4H, br *s*).

*Synthesis of 5,8-dibromoquinoxaline-2,3-diol **(9)***

5,8-Dibromoquinoxaline-2,3-diol **(9)** was synthesized according to the published literature [18, 19]. The product yield was 3.94 g (77 %) of off-white powder. FT-IR (KBr, 4,000–450 cm^{-1}): 3,433 (O–H), 3,091, 3,049 (=C–H). ^{1}H NMR (400 MHz, $CDCl_3$) δ (ppm): 7.73 (2H, *s*), 4.73 (2H, br *s*). Anal. calcd for $C_8H_4Br_2N_2O_2$: C, 30.03; H, 1.26; N, 8.76; found: C, 29.94; H, 1.21; N, 8.85.

Synthesis of metal complexes L1 and L2

The metal complex L1 was synthesized according to [20–22]. Compound **9** (0.62 g, 1.95 mmol) and 2,2′-bipyridine-3,3′-dicarboxylic acid (0.49 g, 2.01 mmol) were dissolved together in methanol (25 mL) with stirring and refluxing. Then a solution of cadmium chloride hemipentahydrate [$CdCl_2{\cdot}2.5H_2O$] (0.46 g, 2.02 mmol) in 25 mL of methanol was added dropwise and refluxing continued for 8 h. The precipitate was collected by filter, washed with methanol and ethanol many times and then dried under vacuum. A gray solid (1.06 g, yield 81 %) was obtained. FT-IR (KBr, 4,000–450 cm^{-1}): 3,224 (–OH), 3,057 (=C–H), 1,692 (C=O), 525 (N–Cd). Anal. calcd for $C_{20}H_{10}Br_2CdN_4O_6$: C, 35.61; H, 1.49; N, 8.31; found: C, 34.76; H, 1.64; N, 8.56 %. L2 was synthesized with the similar synthetic method as L1. L2: (yield: 76 %, 0.97 g). FT-IR (KBr, 4,000–450 cm^{-1}): 3,223 (–OH), 3,066 (=C–H),

1,678 (C=N), 541 (N–Cu). Anal. calcd for $C_{20}H_{10}Br_2CuN_4O_6$: C, 38.39; H, 1.61; N, 8.95; found: C, 37.95; H, 1.73; N, 9.21.

Synthesis of polymeric metal complexes PAL1, PAL2, PBL1 and PBL2

The polymeric metal complex PAL1 was synthesized by the Heck coupling method, according to the literature [23, 24]. A flask was charged with a mixture of L1 (0.85 g, 1.26 mmol), compound **A** (0.55 g, 1.26 mmol), $Pd(OAc)_2$ (0.01 g, 0.06 mmol), tri-*o*-tolylphosphine (0.09 g, 0.29 mmol), DMF (32 mL) and triethylamine (12 mL). The flask was degassed and purged with N_2. The mixture was heated at 90 °C for 36 h under N_2. Then, it was filtered and the filtrate was poured into methanol. The dark brown precipitate was filtered and washed with methanol. The crude product was purified by dissolving in THF and precipitating into methanol to afford a brown solid (yield: 0.76 g, 63 %). FT-IR (KBr, 4,000–450 cm^{-1}): 3,216 (–OH), 3,066 (=C–H), 2,924, 2,858 (C–H), 1,683 (C=O), 534 (N–Cd). Anal. calcd for $C_{51}H_{45}CdN_5O_7$: C, 64.32; H, 4.76; N, 7.35; found: C, 63.07; H, 4.81; N, 7.54 %. Mn = 9.5×10^3 g/mol, PDI = 1.48.

PAL2 was synthesized with the similar synthetic method as PAL1. PAL2: (yield: 0.54 g, 67 %). FT-IR (KBr, 4,000–450 cm^{-1}): 3,224 (–OH), 3,083 (=C–H), 2,932, 2,857 (C–H), 1,681 (C=O), 538 (N–Cu). Anal. calcd for $C_{51}H_{45}CuN_5O_7$: C, 67.80; H, 5.02; N, 7.75; found: C, 66.94; H, 5.43; N, 7.54 %. Mn = 7.2×10^3 g/mol, PDI = 1.51.

PBL1 was synthesized with the similar synthetic method as PAL1. PBL1: (yield: 0.61 g, 74 %). FT-IR (KBr, 4,000–450 cm^{-1}): 3,208 (–OH), 3,057 (=C–H), 2,925, 2,849 (C–H), 1,661 (C=O), 528 (N–Cd). Anal. calcd for $C_{44}H_{37}CdN_5O_6$: C, 62.60; H, 4.42; N, 8.30; found: C, 61.14; H, 4.57; N, 8.02 %. Mn = 10.9×10^3 g/mol, PDI = 1.39.

PBL2 was synthesized with the similar synthetic method as PAL1. PBL2: (yield: 0.47 g, 58 %). FT-IR (KBr, 4,000–450 cm^{-1}): 3,216 (–OH), 3,066 (=C–H), 2,924, 2,849 (C–H), 1,673 (C=O), 542 (N–Cu). Anal. calcd for $C_{44}H_{37}CuN_5O_6$: C, 66.45; H, 4.69; N, 8.81; found: C, 66.19; H, 4.47; N, 8.94 %. Mn = 9.6×10^3 g/mol, PDI = 1.43.

Results and discussion

Synthesis and characterization

The detailed synthetic routes of the four polymeric metal complexes (PAL1, PAL2, PBL1 and PBL2) are shown in Scheme 2, which were synthesized by the Heck coupling reaction [25]. The four as-synthesized polymers could be dissolved in common organic solvents such as DMF and DMSO at room temperature. However, they exhibit a poor solubility in the other solvents, such as in chloroform and dichloromethane.

The Figs. 1 and 2 show the IR spectra of the metal complex L1 and the polymeric metal complexes (PAL1, PBL1), and the metal complex L2 and the polymeric metal

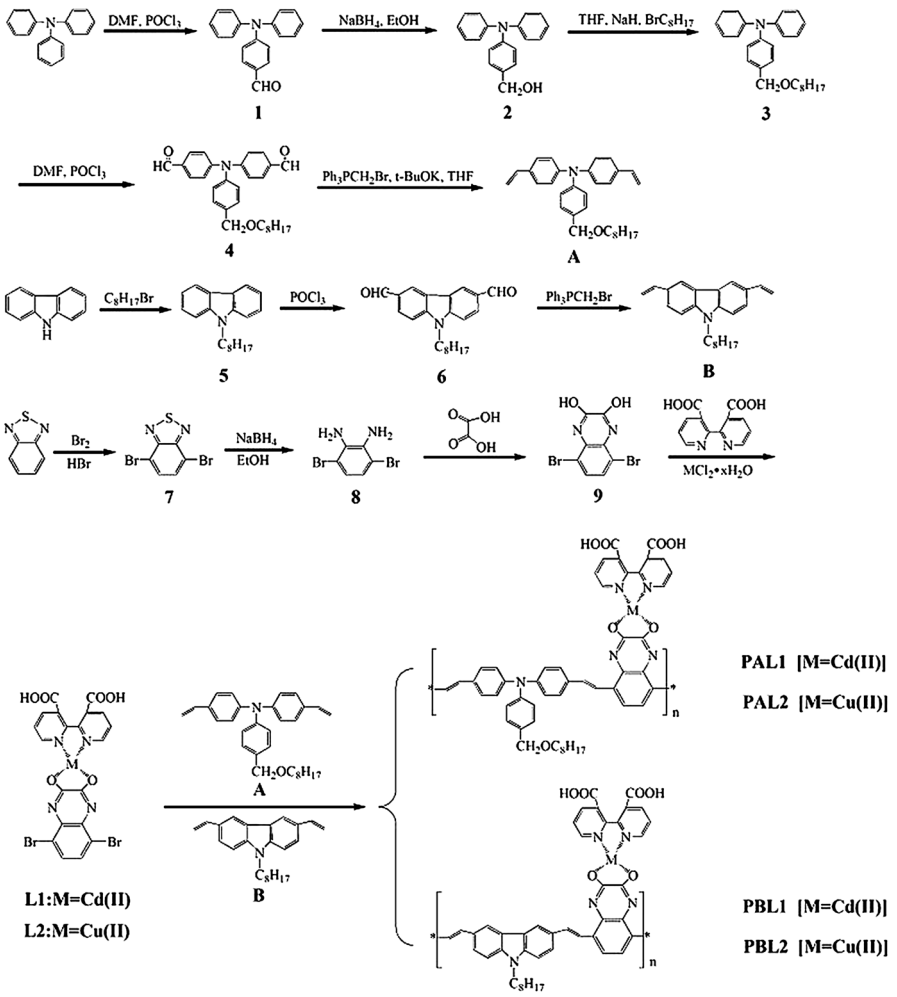

Scheme 2 Synthesis routes for PAL1, PAL2, PBL1 and PBL2

complexes (PAL2, PBL2), respectively. In Fig. 1, as for the metal complex L1, the polymeric metal complexes PAL1 and PBL1 absorption peaks at 3,057, 3,066 and 3,057 cm^{-1} are due to =C–H bond stretching vibration, the peaks of 525, 534 and 528 cm^{-1} are due to N–M bond stretching vibration, respectively [26]. However, the peak at 2,924, 2,858 cm^{-1} of PAL1 and the peak at 2,925, 2,849 cm^{-1} of PBL1 are C–H bond stretching vibration absorption peak. In Fig. 2, the absorption peaks at 3,066, 3,083 and 3,066 cm^{-1} for the metal complex L2, the polymeric metal complexes PAL2 and PBL2, respectively, are due to =C–H bond stretching vibration; the peaks of 541, 538 and 542 cm^{-1} are due to N–M bond stretching vibration [26]. However, the peak at 2,932, 2,857 cm^{-1} of PAL2 and the peak at 2,924, 2,849 cm^{-1} of PBL2 are C–H bond stretching vibration absorption peak.

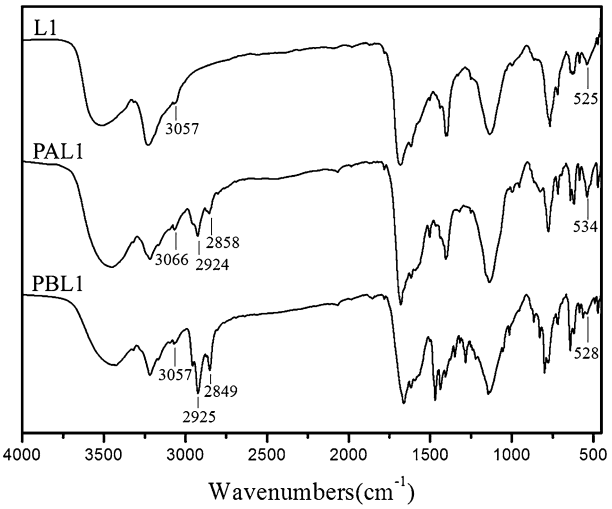

Fig. 1 FT-IR spectra of L1 and polymeric metal complexes (PAL1 and PBL1)

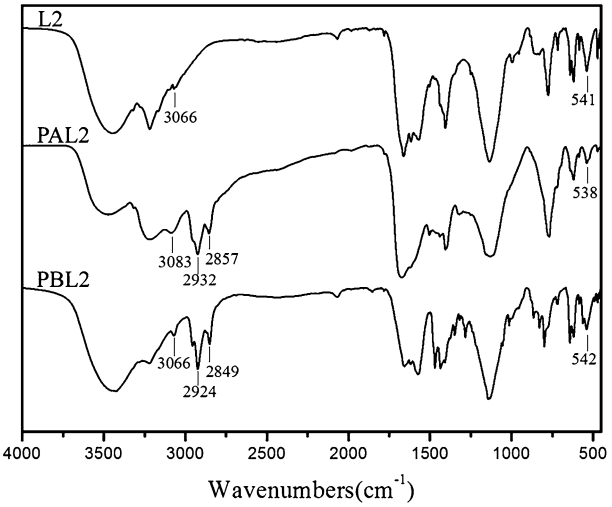

Fig. 2 FT-IR spectra of L2 and polymeric metal complexes (PAL2 and PBL2)

Combining with the results of elemental analysis and the gel permeation chromatography (GPC), we can conclude that the polymeric metal complexes (PAL1, PAL2, PBL1 and PBL2) have been successfully synthesized.

GPC study results of all the target polymers are shown in Table 1. The number average molecular weight of PAL1, PAL2, PBL1 and PBL2 is 9.5, 7.2, 10.9 and 9.6 kg/mol, and the unit of them is 10, 8, 13 and 12, respectively. All the PDI of polymeric metal complexes are relatively wide (PAL1, PAL2, PBL1 and PBL2: 1.48, 1.51, 1.39 and 1.43, respectively).

Table 1 Molecular weights and thermal properties of the polymeric metal complexes

Polymer	$\overline{M}_n$[a] ($\times 10^3$)	$\overline{M}_w$[a] ($\times 10^3$)	N	PDI	T_g[b] (°C)	T_d[c] (°C)
PAL1	9.5	14.1	10	1.48	129	321
PAL2	7.2	10.9	8	1.51	122	302
PBL1	10.9	15.2	13	1.39	141	346
PBL2	9.6	13.7	12	1.43	134	337

[a] Determined by gel permeation chromatography using polystyrene as standard

[b] Determined by DSC with a heating rate of 10 °C/min under nitrogen

[c] The temperature at 5 % weight loss under nitrogen

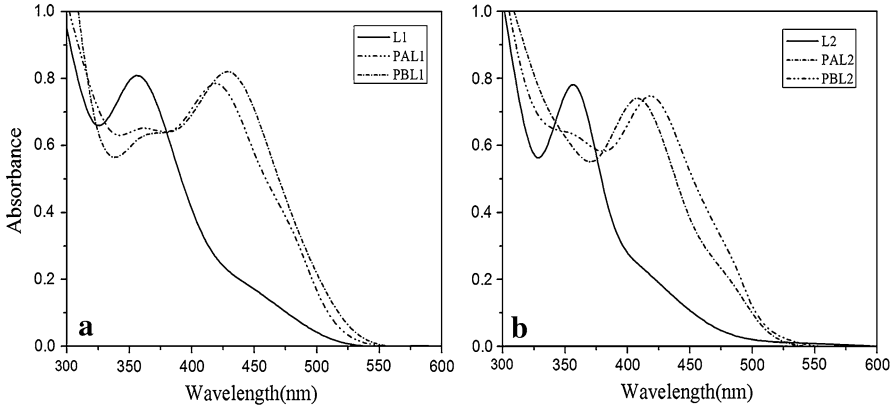

Fig. 3 UV–Vis absorption spectra of L1, L2 and polymeric metal complexes (PAL1, PAL2, PBL1 and PBL2) in DMF solution

Optical properties

Figure 3 gives the UV–Vis spectra of the polymeric metal complexes PAL1, PAL2, PBL1 and PBL2 (10^{-5} M in DMF solution), and the corresponding data are summarized in Table 2.

In Fig. 3, the maximum absorption of PAL1, PAL2, PBL1 and PBL2 are at 422, 408, 431 and 419 nm, respectively, and this absorption bands result from intramolecular charge transfer (ICT) between the electron acceptor metal complex unit and the electron donor alkoxy triphenylamine or octyl carbazole unit. Those polymers have very weak shoulder absorption peak in the band 340–380 nm, which is due to the charge transition of the quinoxaline derivatives and metal ions in the polymer. In comparison with the ligands L1 and L2, the absorption peaks of PAL1, PAL2, PBL1 and PBL2 were red-shifted obviously due to their increasing effective conjugation chain length [27].

The normalized photoluminescent (PL) spectra of PAL1, PAL2, PBL1 and PBL2 are tested in DMF solution, the excitation wavelengths were set according to the absorption peak of UV–Vis spectrum, and the corresponding optical data are also listed in Table 2. It can be seen that the PL peaks of PAL1, PAL2, PBL1 and PBL2

Table 2 Optical and electrochemical properties of the polymeric metal complexes

Polymer	$\lambda^{a}_{a,max}, \lambda^{a}_{a,onset}$	$\lambda^{b}_{p,max}$	E_{ox} (V)[c]	E_{red} (V)[c]	HOMO (eV)	LUMO (eV)	$E_{g,EC}$/eV[d]
PAL1	422,544	477	1.22	−1.04	−5.62	−3.36	2.26
PAL2	408,531	457	1.18	−1.13	−5.58	−3.27	2.31
PBL1	431,556	491	1.21	−1.01	−5.61	−3.39	2.22
PBL2	419,540	473	1.19	−1.09	−5.59	−3.31	2.28

[a] $\lambda_{a,max}$, $\lambda_{a,onset}$: the maxima and onset absorption from the UV–Vis spectra in DMF solution

[b] $\lambda_{p,max}$: the PL maxima in DMF solution

[c] Values determined by cyclic voltammetry

[d] $E_{g,EC}$: electrochemical band gap estimated from HOMO and LUMO

are at 477, 457, 491 and 473 nm, respectively, which maybe result from the strong electron-donating alkoxy group in the side chain [27].

Thermal stability

As an important performance of DSSCs, the dye should have good thermal stability which can increase the thermal stability and effective working time of photovoltaic devices. Therefore, the thermal stability study has important implications for DSSC. TGA and DSC were selected to study the thermal stability of the target product, and the TGA is used to test the target thermal decomposition temperature (T_d: 5 % weight loss temperature), while the DSC is used to test target the glass transition temperature (T_g). The corresponding data are listed in Table 1. The TGA results (Fig. 4) show the T_d of the four polymeric metal complexes (PAL1, PAL2, PBL1 and PBL2) are at temperatures of 321, 302, 346 and 337 °C in nitrogen, respectively, which means all of them are steady [28]. Synchronously, from the data of Table 1, we can see that the T_g of the four polymeric metal complexes (PAL1, PAL2, PBL1 and PBL2) were at 129, 122, 141 and 134 °C respectively, and no crystallization or melting peaks were detected, indicating that the polymers are amorphous. There is no fixed melting point which means that all of target products are amorphous structure and this kind of structure might not be conducive to use in organic solar cells. The high thermal stability of those polymers could benefit to increased stability of the DSSC, preventing morphological change, deformation and degradation of the active layer by current-induced heat during operation of the photovoltaic polymers [29].

Electrochemical properties

Electronic energy level is one of the most important properties for organic materials used in solar cells. Figure 5 shows the cyclic voltammograms of PAL1, PAL2, PBL1 and PBL2. The cyclic voltammetry of polymeric metal complexes was measured in DMF containing $[Bu_4N]BF_4$ (Bu = butyl) as supporting electrolyte and saturated calomel electrode (SCE) as reference electrode at a scan rate of 50 mV/s. The lowest unoccupied molecular orbital (LUMO) and highest occupied molecular

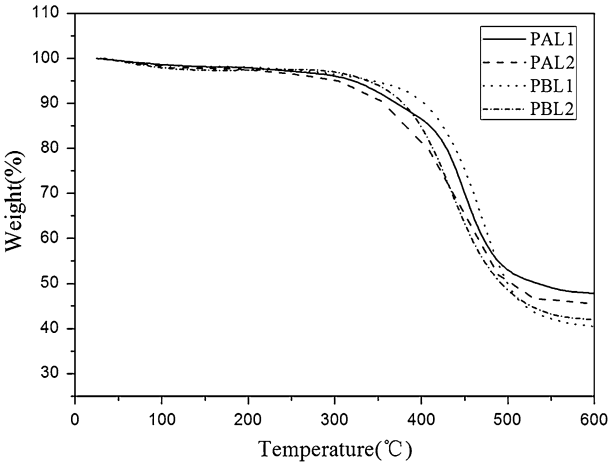

Fig. 4 TGA curves of PAL1, PAL2, PBL1 and PBL2 with a heating rate of 10 °C/min under nitrogen atmosphere

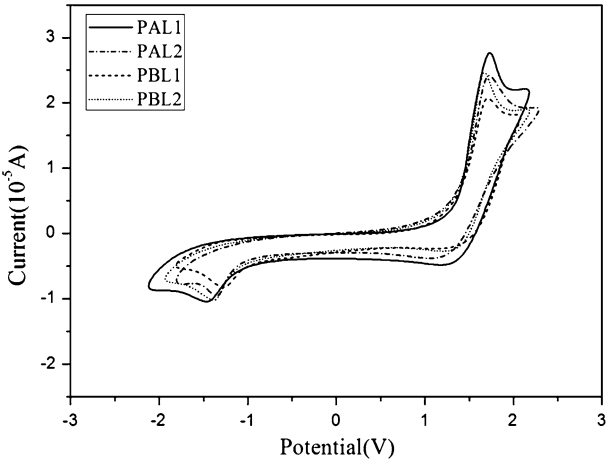

Fig. 5 Cyclic voltammograms for PAL1, PAL2, PBL1 and PBL2 in DMF/0.1 M $[Bu_4N]BF_4$ at 50 mV/s

orbital (HOMO) energy levels of the dyes are crucial property for materials used in DSSC. From the onset oxidation potentials (E_{ox}) and the onset reduction potentials (E_{red}) of the polymers, HOMO and LUMO energy levels as well as the energy gap of the polymers were calculated according to the following equations: [30].

$$E_{HOMO} = -e(E_{ox} + 4.40)\ (eV)$$

$$E_{LUMO} = -e(E_{red} + 4.40)\ (eV)$$

$$E_g = E_{HOMO} - E_{LUMO}.$$

The values obtained are listed in Table 2. The HOMO energy levels of PAL1, PAL2, PBL1 and PBL2 is calculated to be −5.62, −5.58, −5.61 and −5.59 eV, respectively, which are lower than the standard potential of the I_3^-/I^- redox couple (−4.83 eV) [31]. This indicates that sufficient driving forces for the regeneration of the oxidized dyes are available. Their corresponding LUMO energy levels are −3.36, −3.27, −3.39 and −3.31 eV, respectively, and they are sufficiently higher than the conduction band edge of TiO_2 (−4.26 eV) [31], which demonstrate that effective electron transfer from the excited dye to the TiO_2 is ensured.

Photovoltaic properties

DSSC devices based on these four polymeric metal complexes were fabricated and tested under the illumination of AM 1.5 G, 100 mW/cm^2 for solar cell applications. Following our conventional practice for these polymeric metal complexes using solution process [32, 33], the active layers were spin-coated from their DMF solutions. The monochromatic incident photon-to-electron conversion efficiency (IPCE) curves and current–voltage curves (*J*–*V* curves) of the four polymeric metal complexes are shown in Figs. 6 and 7, and the short circuit current (J_{sc}), open circuit voltage (V_{oc}), fill factor (FF) and other relevant data are listed in Table 3.

Figure 6 shows IPCE of the DSSC devices based on four polymeric metal complexes (PAL1, PAL2, PBL1 and PBL2). From the Fig. 6, the IPCE values of the dye PAL1, PAL2, PBL1 and PBL2 reach to 27.51, 28.28, 33.33 and 30.81 %, respectively, around the band 400 nm. Though dye PBL1 has the maximum IPCE among the four dyes, the results are not compared with that of the traditional ruthenium dye, which is probably caused by low charge collection efficiency [34].

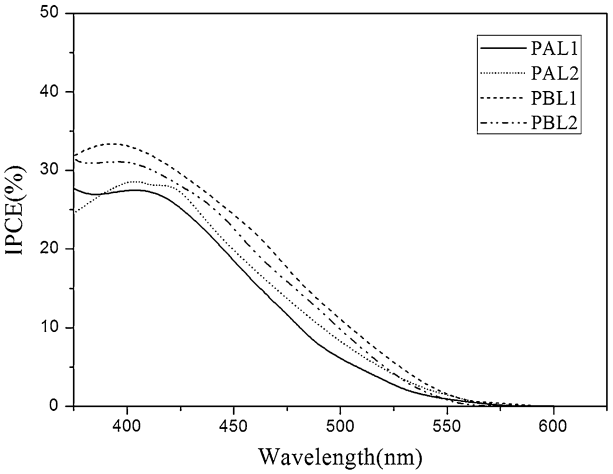

Fig. 6 Monochromatic incident photon-to-electron conversion efficiency (IPCE) curves of DSSCs based on the four polymeric metal complexes (PAL1, PAL2, PBL1 and PBL2)

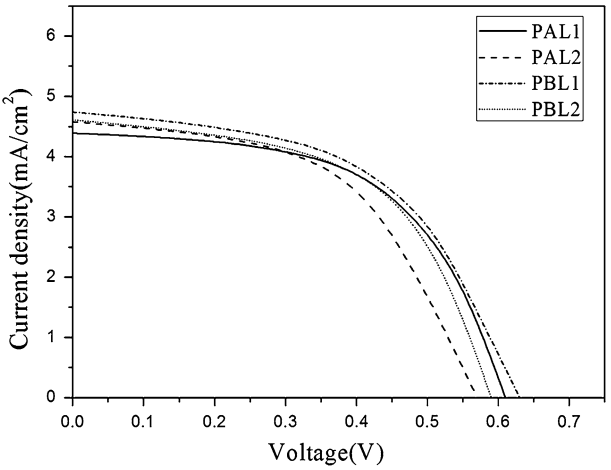

Fig. 7 *J–V* curves of DSSC based on dyes (PAL1, PAL2, PBL1 and PBL2) under the illumination of AM 1.5, 100 mW/cm^2

Table 3 Photovoltaic parameters of devices with sensitizers P1–P4 in DSSCs at full sunlight (AM 1.5 G, 100 mW/cm^2)

Polymer	Solvent	J_{sc} (mA/cm^2)	V_{oc} (V)	FF	η (%)
PAL1	DMF	4.39	0.61	0.62	1.69
PAL2	DMF	4.58	0.57	0.56	1.51
PBL1	DMF	4.74	0.63	0.58	1.76
PBL2	DMF	4.61	0.59	0.60	1.65

The *J–V* curves are reported in Fig. 7 and the corresponding photovoltaic performance is summarized in Table 3. From the data of Table 3, we can see that the short circuit current (J_{sc}) of the PAL1, PAL2, PBL1 and PBL2 is 4.39, 4.58, 4.74 and 4.61 mA/cm^2, respectively, we think the reason for the better photovoltaic properties of polymers with Cd ion than polymers with Cu ion is that the former shows better electron transport ability in D–π–A polymer structure. We may explain this in two factors. First, the radius of Cd^{2+} is bigger than Cu^{2+}; second the extranuclear electron configuration of Cd^{2+} is d^{10} electron configuration, but the Cu^{2+} is not. So the coordination ability of Cd^{2+} is stronger than Cu^{2+}. As a result, the polymers with Cd ion exhibited better photovoltaic properties than the polymers with Cu ion. The reasons for PBL1 having the highest short circuit current among these four polymeric metal complexes are that PBL1 possesses a larger coordinated Cd(II) metal ion and owns higher IPCE, which causes high charge separation and transportation efficiency. The open circuit voltage (V_{oc}) of the PAL1, PAL2, PBL1 and PBL2 is 0.61, 0.57, 0.63 and 0.59 V, respectively. The power conversion efficiency (η) based on PAL1, PAL2, PBL1 and PBL2 reached 1.69, 1.51, 1.76 and 1.65 %, respectively.

Conclusions

In summary, four novel polymeric metal complexes were successfully synthesized and characterized by IR, ^{1}H NMR, Gel permeation chromatography (GPC), elemental analysis and so on. Their photovoltaic performances in DSSCs were also investigated. The target products have showed good thermal stability, higher open circuit voltages and some power conversion efficiency. There are still many challenges to obtain outstanding power conversion efficiency; the weak adsorption affinities on the TiO_2, high energy band gap, inefficient light absorption and ICT are the main reasons that we cannot obtain outstanding efficiency [35].

As next work, there are still many challenges to obtaining outstanding PCE, especially the low J_{sc} based on the materials, narrow absorption spectra of the polymers and no adsorption affinities on the surface of TiO_2. For strong adsorption onto the surface of TiO_2, anchoring groups should also be introduced in the structure. This work provides a new path for the study and design of the new practical dye sensitizers.

References

1. Wang J, Cong S, Wen S, Yan L, Zhongmin S (2013) A rational design for dye sensitizer: density functional theory study on the electronic absorption spectra of organoimido-substituted hexamolybdates. J Phys Chem C 117:2245–2251
2. Ronnen L, Paul B, Hashem A (2005) Solar spectral optical properties of pigments-part I: model for deriving scattering and absorption coefficients from transmittance and reflectance measurements. Sol Energy Mater Sol Cells 89:319–349
3. O'Regan B, Grätzel M (1991) A low-cost, high-efficiency solar cell based on dye-sensitized colloidal TiO_2 films. Nature 353:737–740
4. Xuefeng L, Feng Q, Lan T, Zhou G, Wang Z-S (2012) Molecular engineering of quinoxaline-based organic sensitizers for highly efficient and stable dye-sensitized solar cells. Chem Mater 24:3179–3187
5. Mishra A, Markus Fischer KR, Bäuerle P (2009) Metal-free organic dyes for dye-sensitized solar cells: from structure: property relationships to design rules. Angew Chem Int Ed 48:2474–2499
6. Jin X, Deng J, Wen G, Xiaoguang Y, Zhong C (2013) Synthesis and photovoltaic properties of main chain polymeric metal complexes containing 1,10-phenanthroline metal complexes conjugating alkyl fluorene or alkoxy benzene by C=C bridge for dye-sensitized solar cells. Polym Adv Technol 24:266–269
7. Williams KA, Boydston AJ, Bielawski CW (2007) Main-chain organometallic polymers: synthetic strategies, applications, and perspectives. Chem Soc Rev 36:729–744
8. Leung ACW, Chong JH, Patrick BO, Mark MacLachlan J (2003) Poly (salphenyleneethynylene) s: a new class of soluble, conjugated, metal-containing polymers. Macromolecules 36:5051–5054
9. Wang X-M, Zhou Y-F, Wen-Tao Y, Wang C, Fang Q, Jiang M-H, Lei H, Wang H-Z (2000) Two-photon pumped lasing stilbene-type chromophores containing various terminal donor groups: relationship between lasing efficiency and intramolecular charge transfer. J Mater Chem 10:2698–2703
10. Lee J, Jung B-J, Lee J-I, Chu HY, Do L-M, Shim H-K (2002) Modification of an ITO anode with a hole-transporting SAM for improved OLED device characteristics. J Mater Chem 12:3494–3498
11. Liu B, Zhang Q, Ding H, Guiju H, Yajun D, Wang C, Jieying W, Li S, Zhou H, Yang J, Tian Y (2012) Synthesis, crystal structures and two-photon absorption properties of a series of terpyridine-based chromophores. Dyes Pigment 95:149–160
12. Juan P, Mao L, Jun C, Zhanliang T, Wei X (2008) Application of triphenylamine-based sensitizers with two carboxylic acid groups to dye-sensitized solar cells. Acta Phys Chim Sin 24:1950–1956

13. Zhu Y, Rabindranath AR, Beyerlein T, Tieke B (2007) Highly luminescent 1,4-diketo-3,6-diphenylpyrrolo[3,4-c]pyrrole-(DPP-) based conjugated polymers prepared upon Suzuki coupling. Macromolecules 40:6981–6989
14. He A, Zhong C, Huang H, Zhou Y, He Y, Zhang H (2008) Synthesis and luminescent properties of Cu(II), Zn(II) polymeric complexes with electron- and hole-transporting groups. J Lumin 128:1291–1296
15. He Y, Zhong C, Zhou Y, He A, Zhang H (2009) Synthesis and luminescent properties of novel bisfunctional polymeric complexes based on carbazole and 8-hydroxyquinoline groups. Mater Chem Phys 114:261–266
16. Morin J-F, Drolet N, Tao Y, Leclerc M (2004) Syntheses and characterization of electroactive and photoactive 2,7-carbazolenevinylene-based conjugated oligomers and polymers. Chem Mater 16:4619–4626
17. Kim J, Park SH, Kim J, Cho S, Jin Y, Shim JY, Shin H, Kim I, Kwon S, Lee K, Heeger AJ, Suh H (2011) Syntheses and characterization of carbazole based new low-band gap copolymers containing highly soluble benzimidazole derivatives for solar cell application. J Polym Sci Part A Polym Chem 49:369–380
18. Sonawane YA, Rajule RN, Shankarling GS (2010) Synthesis of novel diphenylamine-based fluorescent styryl colorants and study of their thermal, photophysical, and electrochemical properties. Monatsh Chem 141:1145–1151
19. Romer DR (2009) Synthesis of 2,3-dichloroquinoxalines via Vilsmeier reagent chlorination. J. Heterocycl Chem 46:317–319
20. Zhang L, Wen G, Xiu Q, Guo L, Deng J, Zhong C (2012) Synthesis and photovoltaic properties of polymeric metal complexes containing 8-hydroxyquinoline as dye sensitizers for dye-sensitized solar cells. J Coord Chem 65:1632–1644
21. Xiao L, Liu Y, Xiu Q, Zhang L, Guo L, Zhang H, Zhong C (2010) Novel polymeric metal complexes as dye sensitizers for dye-sensitized solar cells based on poly thiophene containing complexes of 8-hydroxyquinoline with Zn(II), Cu(II) and Eu(III) in the side chain. Tetrahedron 66:2835–2842
22. Xiao L, Liu Y, Xiu Q, Zhang L, Guo L, Zhang H, Zhong C (2010) Two main chain polymeric metal complexes as dye sensitizers for dye-sensitized solar cells based on the coordination of the ligand containing 8-hydroxyquinoline and phenylethyl or fluorene units with Eu(III). J Polym Sci Part A Polym Chem 48:1943–1951
23. Tsai L-R, Chen Y (2008) Hyperbranched and thermally cross-linkable oligomer from a new 2,5,7-trifunctional fluorene monomer. J Polym Sci Part A Polym Chem 46:70–84
24. Deng J, Xiu Q, Guo L, Zhang L, Wen G, Zhong C (2012) Branched chain polymeric metal complexes containing Co(II) or Ni(II) complexes with a donor–π–acceptor architecture: synthesis, characterization, and photovoltaic applications. J Mater Sci 47:3383–3390
25. Ziegler Jr CB, Heck RF (1978) Palladium-catalyzed vinylic substitution with highly activated aryl halides. J Org Chem 43:2941–2946
26. Liu Y, Xiu Q, Xiao L, Huang H, Guo L, Zhang L, Zhang H, Tan S, Zhong C (2011) Two novel branched chain polymeric metal complexes based on Cd(II), Zn(II) with fluorene, thiophene, 8-hydroxyquinoline, and 1,10-phenathroline ligand: synthesis, characterization, photovoltaic properties, and their application in DSSCs. Polym Adv Technol 22:2583
27. Xiaoguang Y, Wen G, D Jinyan, Jin X, Zhou J, Zhang W, Zhong C (2013) Novel main chain polymeric metal complexes based on Zn(II) or Cd(II) with fluorene and 8-hydroxyquinoline ligand: synthesis, characterization and photovoltaic application in DSSCs. J Inorg Organomet Polym 23:579–586
28. Jin SH, Park HJ, Kim JY, Lee K, Lee SP, Moon DK, Lee HJ, Gal YS (2003) Synthesis and electroluminescence properties of poly (9, 9-di-*n*-octylfluorenyl-2, 7-vinylene) derivatives for light-emitting display. Macromolecules 35:7532
29. Bertho S, Haeldermans I, Swinnen A, Moons W, Martens T, Lutsen L, Vanderzande D, Manca J, Senesc A, Bonfiglio A (2007) Influence of thermal ageing on the stability of polymer bulk heterojunction solar cells. Sol Energy Mater Sol Cells 91:385–389
30. Wang L-H, Kang E-T, Chen BJ, Lee CS, Lee ST, Chen Z-K, Huang W (2000) A family of electroluminescent silyl-substituted poly(*p*-phenylenevinylene)s: synthesis, characterization, and structure-property relationships. Macromolecules 33:9015–9025
31. Zhang L, Cole JM, Waddell PG, Low KS, Liu X (2013) Relating electron donor and carboxylic acid anchoring substitution effects in azo dyes to dye-sensitized solar cell performance. ACS Sustain Chem Eng 11:1440–1452

32. Liu Y, Wan X, Wang F, Zhou J, Long G, Tian J, You J, Yang Y, Chen Y (2011) Adv Energy Mater 1:771–775
33. He G, Li Z, Wan X, Liu Y, Zhou J, Long G, Zhang M, Chen Y (2012) Small molecules based on benzo [1, 2-b: 4, 5-b'] dithiophene unit for high-performance solution processed organic solar cells. J Mater Chem 22:9173–9180
34. Fischer MKR, Wenger S, Wang M, Mishra A, Zakeeruddin SM, Gratzel M, Bauerle P (2010) D–π–A sensitizers for dye-sensitized solar cells: linear vs branched oligothiophenes. Chem Mater 22:1836–1845
35. Wang Z-S, Li F-Y, Huang C-H (2001) Photocurrent enhancement of hemicyanine dyes containing RSO_3^- group through treating TiO_2 films with hydrochloric acid. J Phys Chem B 105:9210–9217